A photoactivatable small-molecule inhibitor for light-controlled spatiotemporal regulation of Rho kinase in live embryos

Allison R. Morckel[1], Hrvoje Lusic[2], Laila Farzana[1], Jeffrey A. Yoder[1,3], Alexander Deiters[2,3] and Nanette M. Nascone-Yoder[1,3,*]

SUMMARY

To uncover the molecular mechanisms of embryonic development, the ideal loss-of-function strategy would be capable of targeting specific regions of the living embryo with both temporal and spatial precision. To this end, we have developed a novel pharmacological agent that can be light activated to achieve spatiotemporally limited inhibition of Rho kinase activity in vivo. A new photolabile caging group, 6-nitropiperonyloxymethyl (NPOM), was installed on a small-molecule inhibitor of Rho kinase, Rockout, to generate a 'caged Rockout' derivative. Complementary biochemical, cellular, molecular and morphogenetic assays in both mammalian cell culture and *Xenopus laevis* embryos validate that the inhibitory activity of the caged compound is dependent on exposure to light. Conveniently, this unique reagent retains many of the practical advantages of conventional small-molecule inhibitors, including delivery by simple diffusion in the growth medium and concentration-dependent tuneability, but can be locally activated by decaging with standard instrumentation. Application of this novel tool to the spatially heterogeneous problem of embryonic left-right asymmetry revealed a differential requirement for Rho signaling on the left and right sides of the primitive gut tube, yielding new insight into the molecular mechanisms that generate asymmetric organ morphology. As many aromatic/heterocyclic small-molecule inhibitors are amenable to installation of this caging group, our results indicate that photocaging pharmacological inhibitors might be a generalizable technique for engendering convenient loss-of-function reagents with great potential for wide application in developmental biology.

KEY WORDS: Small-molecule inhibitor, Rho kinase, Photocaging, *Xenopus*

INTRODUCTION

Small-molecule inhibitors are increasingly utilized as loss-of-function tools to investigate mechanisms of development. Their ease of delivery, reversibility, concentration-dependent phenotypes and cross-species activity have made these compounds invaluable for investigating the role of specific signaling pathways in dynamic morphogenetic processes including organogenesis and regeneration (e.g. Mathew et al., 2009; Moura et al., 2011). Although small molecule exposure can be limited to precise developmental windows, the effects are not spatially restricted, limiting their utility for studies of a specific region of interest within the context of the whole embryo.

Effective spatiotemporal control of biologically active molecules has been achieved by the addition of 'caging' groups installed via a photocleavable bond on a key substituent essential for activity. The caging group hinders function until the molecule is liberated, or 'decaged', by exposure to a specific wavelength of light (Ellis-Davies, 2007; Deiters, 2010). Although photoactivatable reagents have been used successfully in live embryos, existing methodologies require caged reagents to be delivered by microinjection (Shestopalov et al., 2007; Deiters et al., 2010), work only in the context of a properly engineered fusion protein (e.g. Sinha et al., 2010), and/or function in a transgenic context (Wang et al., 2010; Cambridge et al., 2009), thus limiting their general utility. By contrast, caged pharmacological inhibitors that are deliverable by passive diffusion and that target evolutionary conserved cell signaling proteins would be broadly applicable for the analysis of protein function during development.

One protein that would be desirable to target with such a reagent is RhoA. Rho family GTPases play roles in many morphogenetic events including cell rearrangement, tissue elongation, organogenesis and epithelial morphogenesis (Kim and Han, 2005; Lai et al., 2005; Thumkeo et al., 2005). Rho signals via Rho-associated kinases (Riento and Ridley, 2003), and small-molecule Rho kinase inhibitors [e.g. Y27632 (Aznar et al., 2004; Tamura et al., 2005)] have been developed to specifically inhibit this important signaling component. Numerous research endeavors have relied on these inhibitors to reveal the role of Rho signaling in various morphogenetic contexts in different species (He et al., 2010; Sherrard et al., 2010; Simoes et al., 2010; Wei et al., 2001; Remond et al., 2006), as well as in regeneration and stem cell biology (Cadotte and Fehlings, 2011; Watanabe, 2010; Rizzino, 2010). Here, we report the engineering and application of a photoactivatable small-molecule inhibitor of Rho kinase.

MATERIALS AND METHODS

Synthesis of caged Rockout

Sodium hydride (15 mg, 0.61 mmol) was added to a solution of 3-(4-pyridyl)-1*H*-indole [Rockout, RO (Yarrow et al., 2005)] (100 mg, 0.51 mmol) in DMF (1 ml) at 0°C. The reaction was stirred for 1 hour at 0°C.

[1]Department of Molecular Biomedical Sciences, College of Veterinary Medicine, 1051 William Moore Drive, North Carolina State University, Raleigh, NC 27606, USA. [2]Department of Chemistry, North Carolina State University, Raleigh, NC 27695, USA. [3]Center for Comparative Medicine and Translational Research, North Carolina State University College of Veterinary Medicine, 1060 William Moore Drive, Raleigh, NC 27607, USA.

*Author for correspondence (nmnascon@ncsu.edu)

The solution was cooled to –78°C, followed by the addition of 6-nitropiperonyloxymethyl chloride [NPOM-Cl (Lusic and Deiters, 2006)] (158 mg, 0.61 mmol) in DMF (0.3 ml). The reaction was stirred for 12 hours at room temperature, quenched by the addition of saturated NaHCO$_3$ (1 ml), diluted with ethyl acetate (10 ml) and washed with water (10 ml) and saturated NaCl (10 ml). The organic layer was dried over Na$_2$SO$_4$, filtered and concentrated under vacuum; residue was purified by silica gel chromatography using hexanes:ethyl acetate (7:3, containing 1% triethanolamine), affording 1-{[1-(6-nitrobenzo[d][1,3]dioxol-5-yl)ethoxy]methyl}-3-(pyridin-4-yl)-1H-indole (caged Rockout, cRO) in 47% yield as a brown solid (97 mg, 0.23 mmol). For full characterization, see supplementary material Fig. S1.

Embryos
Experiments complied with all institutional and national animal welfare laws. In vitro fertilization, culture in 0.1× MMR, and staging of *X. laevis* were as described (Sive et al., 1998; Nieuwkoop and Faber, 1994). Synthetic RNA encoding Eos was synthesized using the mMessage mMachine kit (Ambion) via the pEosFP-CS2 plasmid [gift of S. Wacker (Wacker et al., 2007)] and injected in ventro-vegetal blastomeres at the 8-cell stage to serve as a lineage tracer for UV exposure.

In vivo decaging
Stage 35-39 embryos were exposed to 1-40 µM cRO in 0.1× MMR or the equivalent volume of DMSO for 60-270 minutes in a light-proof chamber, rinsed in 0.1× MMR, exposed to UV (focused via a Zeiss Lumar stereomicroscope, DAPI filter, 150 W mercury bulb) for 30-120 seconds, and cultured in 0.1× MMR in the dark until stage 46. Tadpoles were anesthetized in 0.05% MS222 (Sive et al., 1998).

Immunohistochemistry
Stage 45/46 embryos were fixed, embedded, cryosectioned and stained as previously described (Reed et al., 2009) using anti-β-catenin (Sigma, C2206; 1:200) and anti-smooth muscle actin (Sigma, A5228; 1:1000) antibodies.

Decaging in cells
NIH3T3 cells (ATCC number CRL-1658) were grown in DMEM containing 10% bovine serum and antibiotics at 37°C, 5% CO$_2$. Cells were grown in four-chamber slides to 70% confluency and starved overnight in 0.1% serum before being exposed to 40 µM RO or cRO for 10-15 minutes in light-proof chambers. Cells were then rinsed in PBS, exposed to 365 nm UV light (Spectroline lamp) for 10 minutes, and then cultured for 15 minutes before fixation (4% paraformaldehyde) and permeabilization (0.1% Triton X-100). Actin was visualized with Alexa Fluor 488-phalloidin.

Rho kinase assay
Rho kinase activity was measured by the ability of purified human Rho kinase to phosphorylate threonine 696 on the myosin-binding subunit of myosin phosphatase using an ELISA-based kit (Cyclex, CY-1160).

RESULTS AND DISCUSSION
Synthesis of photoactivatable Rho kinase inhibitor
Heterocyclic rings are widely used as the core scaffold of small-molecule inhibitors of important biological targets. We recently developed a new photocaging group for such compounds, 6-nitropiperonyloxymethyl (NPOM), that yields stably caged *N*-heterocyclic molecules under physiological conditions but readily decages upon exposure to non-photodamaging 365 nm ultraviolet (UV) light (Lusic et al., 2007; Lusic and Deiters, 2006). We have shown that this photolabile group can be effectively and safely decaged in live embryos using a fluorescence microscope, UV LED fiber optic instruments or a hand-held UVA lamp (Deiters et al., 2010).

To test the feasibility of using this protecting group to generate photoactivatable pharmacological inhibitors, we generated a caged version of 3-(4-pyridyl)-1H-indole or Rockout (RO) (Yarrow et al., 2005), an inhibitor of Rho kinase with an *N*-heterocyclic core
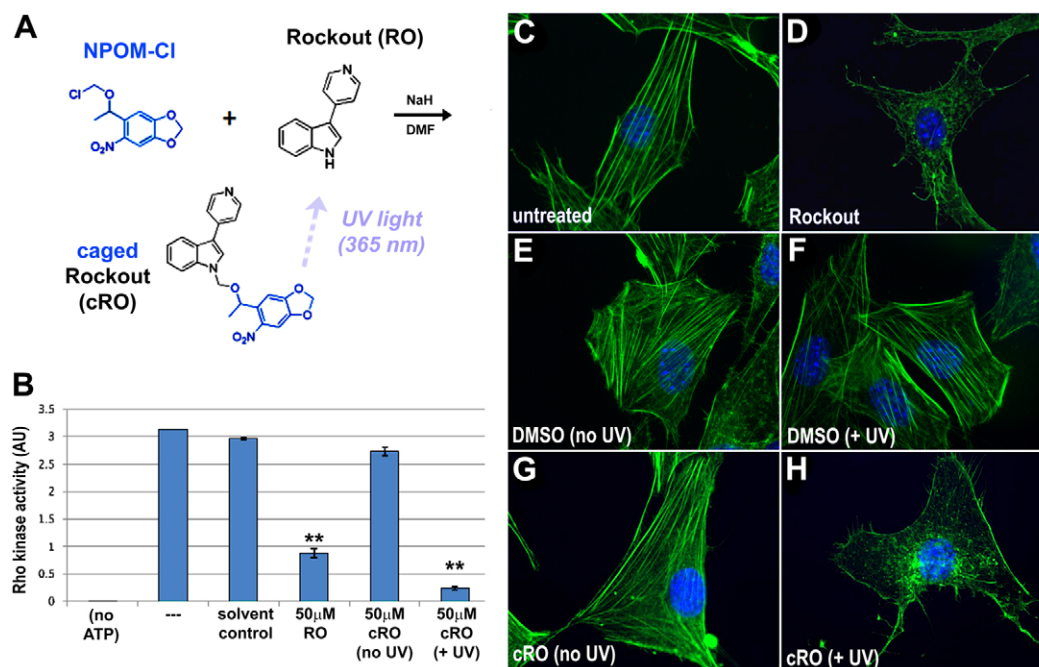

Fig. 1. Synthesis of a photoactivatable Rho kinase inhibitor. (**A**) Caged Rockout (cRO) was generated by installing 6-nitropiperonyloxymethyl (NPOM) on the indole nitrogen of Rockout (RO). Exposure to UV light releases the NPOM caging group, restoring Rho kinase inhibitory activity. (**B**) Rho kinase activity was assayed in vitro using a Rho kinase assay, under standard conditions (---) or in the presence of DMSO (solvent control), 50 µM RO, or 50 µM cRO with (+ UV) and without (no UV) irradiation. The assay was also run without ATP as a negative control (no ATP). The data shown are representative of several independent trials; in the trial shown, the effect of cRO + UV is slightly greater than the effect of RO itself ($P<0.05$), but this result was not consistently observed. **, $P<0.01$ (one-way ANOVA); error bars indicate s.d. (**C-H**) NIH3T3 cells were untreated (C) or exposed to RO (D), DMSO (E,F) or cRO (G,H) and left in the dark (C-E,G) or exposed to UV irradiation (F,H). Blue, DAPI; green, phalloidin.
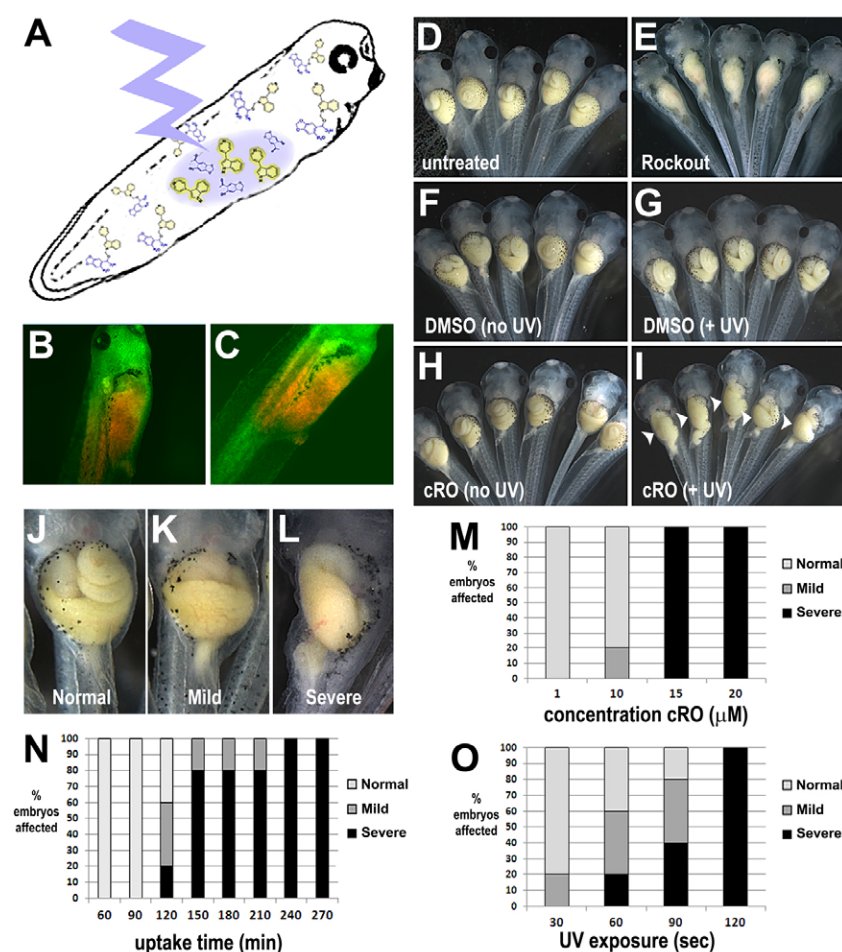
Fig. 2. In vivo efficacy of caged Rockout.
(**A-C**) Stage 39 *Xenopus* embryos were exposed to 40 µM cRO for 2 hours, rinsed and individually irradiated on the right-hand side of the prospective gut (A); green-to-red photoconversion of EosFP indicates the decaged region (B, ventral view; C, right view). (**D-I**) Irradiated groups were then cultured in embryo medium (0.1× MMR) in the dark until the end of gut morphogenesis (stage 46). Embryos grown in the dark in 0.1× MMR (untreated, D), DMSO (F) or cRO (H) have long coiled guts, compared with those cultured in 30 µM RO (E), which have uniformly straight, un-elongated guts. Right side UV irradiation does not affect gut morphology in DMSO controls (G), but induces regions of defective elongation on the right side of the gut (arrowheads) in cRO-exposed embryos (I). (**J-O**) The proportion of normal (J), mild (K) and severe (L) gut elongation defects induced by decaging of cRO is dependent on the concentration of cRO to which the embryos are exposed (120 minutes uptake, 60 seconds irradiation; M), the uptake time (15 µM cRO, 60 seconds irradiation; N), and the length of UV irradiation (15 µM cRO, 120 minutes uptake; O). Control embryos may be exposed to UV for up to 2 minutes or cRO for up to 240 minutes (non-irradiated) without adverse effect (not shown).

structure (Fig. 1A). We installed NPOM on the indole nitrogen, a substituent previously shown to be required for Rho kinase inhibitory activity (Yarrow et al., 2005), yielding NPOM-caged Rockout (cRO) (Fig. 1A; see Materials and methods). The caged compound proved resistant to hydrolysis under physiological conditions (supplementary material Fig. S2). In vitro decaging confirmed UV-dependent disappearance of the caged substrate and recovery of the decaged molecule (supplementary material Fig. S3). As expected, in the absence of UV light cRO has a negligible effect on Rho kinase activity (Fig. 1B). By contrast, after UV exposure (~365 nm), Rho kinase activity is inhibited by 91.2%, confirming that cRO effectively inhibits Rho kinase signaling in a light-dependent manner.

Caged Rockout is cell permeable and its inhibitory activity is light dependent

Rockout was discovered in a cell-based screen (Yarrow et al., 2005) in which it was found to disrupt actin polymerization, promoting the loss of stress fibers and generation of ruffling protrusions. To validate the efficacy of our NPOM-caged version of this compound in vivo, we assessed these actin-dependent morphologies in an uncaging experiment with cultured cells. Serum-starved NIH3T3 cells were exposed to cRO for 10 minutes and rinsed prior to irradiation to eliminate any cRO that had not been taken up by passive diffusion. Importantly, cells exposed to cRO but cultured in the dark exhibited normal actin architecture (Fig. 1G, supplementary material Fig. S4D), comparable to that of

untreated cells (Fig. 1C, supplementary material Fig. S4A) and DMSO-treated controls (Fig. 1E, supplementary material Fig. S4B), thus confirming the lack of background cRO activity in the absence of light, a vital prerequisite for light-activation experiments. By contrast, upon exposure of cRO-treated cells to UV light, stress fiber formation was dramatically reduced and irradiated cells exhibited ruffling protrusions (Fig. 1H, supplementary material Fig. S4E), similar to the defects induced by exposure to conventional RO (Fig. 1D, supplementary material Fig. S4F). Importantly, light-induced changes were not observed in DMSO controls (Fig. 1F, supplementary material Fig. S4C), confirming that these effects are not due to phototoxicity. Thus, cRO is both cell permeable and exhibits light-dependent Rho kinase inhibitory activity in cell culture.

Caged Rockout activity is light dependent in whole embryos

To determine whether the caged Rho kinase inhibitor can permeate complex tissues and exert light-dependent activity in whole embryos, tailbud stage *Xenopus* were exposed to cRO. After equilibration in 40 µM cRO, liquid chromatography/mass spectrometry analysis confirmed effective uptake of the caged compound into embryonic tissues (intra-embryonic concentration, 45 µM; supplementary material Table S1). Importantly, when cultured in the dark, the treated embryos exhibited completely normal morphology (compare Fig. 2D with 2H), showing that cRO is non-toxic and exhibits no background inhibitory activity.
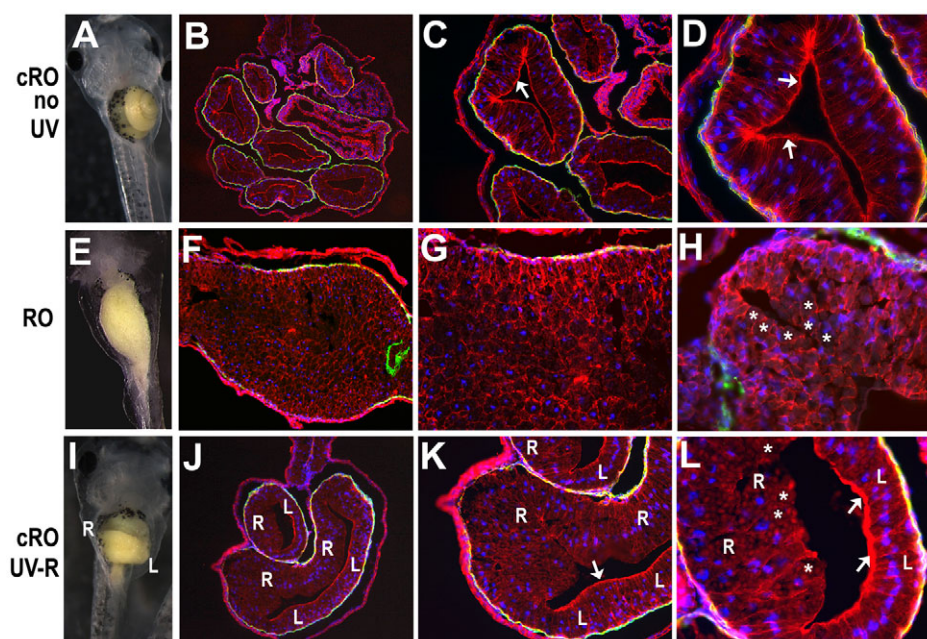
Fig. 3. Caged Rockout locally affects gut epithelial morphogenesis in a light-dependent manner. (A-L) Stage 39 *Xenopus* embryos were exposed to cRO (A-D,I-L), rinsed and kept in the dark (A-D) or irradiated on the right-hand side (I-L), as in Fig. 2. Stage 46 embryos (A,E,I) were sectioned and stained for β-catenin (red) and smooth muscle actin (green); DAPI (blue) indicates nuclei. In contrast to the single-layer columnar epithelium in control (non-irradiated) embryos (B-D), epithelial architecture on the irradiated right side of cRO-treated embryos is highly stratified and disorganized ('R' in J-L), similar to that observed throughout the gut in embryos globally exposed to RO (F-H). In non-irradiated embryos, and on the non-irradiated left ('L') side of cRO-treated embryos, β-catenin is concentrated at the apical surface of the columnar epithelium (arrows in C,D,K,L). By contrast, very little β-catenin appears apically localized in RO guts (asterisks in H) or within the irradiated right side ('R') of cRO-treated guts (asterisks in L). B,F,J, 100×; C,G,K, 200×; D,H,L, 400×.

We previously showed that Rho kinase inhibitors perturb the elongation of the primitive gut tube in *Xenopus* (Reed et al., 2009). Therefore, to validate that cRO can be effectively decaged in vivo, we assessed its ability to induce localized gut elongation defects. After equilibration in 40 μM cRO, embryos were rinsed in normal growth medium (0.1× MMR) to eliminate any cRO that had not been taken up by passive diffusion, anesthetized in MS222, and placed on their left side. They were then individually irradiated (or mock irradiated) for 1 minute with UV light to photoactivate cRO on only the right-hand side of the prospective gut tube (Fig. 2A), and subsequently cultured in 0.1× MMR until stage 46. Irradiated areas were verified by green-to-red photoconversion of EosFP (Fig. 2B,C; see Materials and methods).

Irradiated cRO-treated embryos exhibited defects in gut elongation that were comparable in severity to those induced by global application of Rho kinase inhibitors (Reed et al., 2009) (Fig. 2E), but, remarkably, the abnormal morphogenesis was localized to the irradiated side, yielding novel, unilaterally shortened gut phenotypes (Fig. 2I). Importantly, both irradiated and non-irradiated control embryos exposed to DMSO developed normal gut morphology, confirming that the deformities are not elicited by UV exposure alone (Fig. 2F,G). Additional control experiments indicate that the release of the NPOM caging group itself is not responsible for the observed phenotype (not shown), consistent with our previous observations that NPOM is non-toxic in embryos (Deiters et al., 2010). Importantly, the UV-induced gut phenotypes in cRO-treated embryos correlate with a significant (88-91%) decrease in the intra-embryonic concentration of cRO, accompanied by a significant (14- to 17-fold) increase in the intra-embryonic concentration of decaged RO (supplementary material Table S1).

Gut phenotypes of varying severity (Fig. 2J-L) can be obtained by varying the concentration of cRO in the media (Fig. 2M), the equilibration/uptake time (Fig. 2N) and/or the duration of UV exposure (Fig. 2O). These results demonstrate the remarkable tuneability of this reagent. Here, 150 minutes of uptake at 15 μM cRO, followed by 60 seconds of irradiation, proved optimal; however, these adjustable parameters can be optimized for different species, stages or developmental processes.

Caged Rockout induces light-dependent localized Rockout phenotypes

To confirm that cRO can fully phenocopy the expected morphogenetic effects of Rho kinase inhibition, unilateral gut defects were analyzed at the tissue and cellular level. We found previously (Reed et al., 2009) that global exposure to RO leads to aberrant cell rearrangements and abnormal epithelial morphogenesis in the shortened gut tube (compare Fig. 3A-D with 3E-H). As expected, the irradiated, decaged side of cRO-exposed guts exhibited similar defects in cellular architecture, including failure to form a single-layer epithelium and to apically localize β-catenin (Fig. 3I-L, right side epithelia), comparable to the defects induced globally by RO (Reed et al., 2009) (Fig. 3E-H). By contrast, the non-irradiated side of cRO-exposed guts had completely normal epithelial architecture (e.g. compare left side epithelium in Fig. 3J-L with 3B-D). The irradiated gut cells also failed to undergo the normal tissue-elongating rearrangements observed in control embryos (supplementary material Fig. S5). Thus, cRO phenocopies RO at the organ, tissue and cellular level in a light-dependent and spatially localized manner.
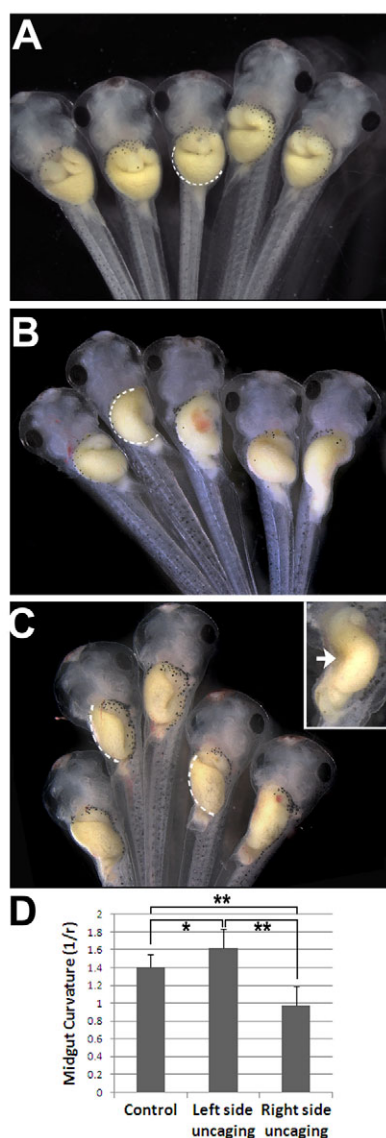
Fig. 4. Rho kinase plays different roles on contralateral sides of the gut. (**A-C**) Stage 38 *Xenopus* embryos were exposed to cRO, rinsed, and kept in the dark (A) or irradiated on the left (B) or right (C) side of the prospective gut, as in Fig. 2. The arc of the midgut curvature is indicated by the dashed line. Inset (C) shows a reversed curvature caused by ectopic concavity (arrow). (**D**) Average curvature for each condition ($n \geq 10$) was quantified as 1/radius of the best-fit circle superimposed on the greater curvature of the midgut. *, $P<0.05$; **, $P<0.01$ (one-way ANOVA); error bars indicate s.d.

Caged Rockout reveals a side-specific role for Rho kinase in left-right asymmetric morphogenesis

The *Xenopus* gut develops a prominent rightward curvature that initiates intestinal rotation. The direction of this asymmetry is dependent on early left-right asymmetric gene expression (Ibanes and Izpisua Belmonte, 2009), but the specific morphogenetic mechanisms that shape gut curvature are largely unknown. It has been reported that the right side of the midgut elongates more rapidly than the left (Muller et al., 2003), suggesting that asymmetric tissue elongation could generate this important morphological asymmetry. Since Rho signaling regulates gut elongation there might be unequal requirements for Rho kinase on

the left and right sides of the gut tube. If so, disrupting Rho kinase activity on the more rapidly elongating right side would be expected to equalize the rate of elongation on the two sides, reducing or eliminating the curvature. By contrast, disruption of Rho kinase activity on the left would be predicted to have no effect on the direction of curvature as this would merely enhance the existing asymmetry in tissue elongation.

We employed cRO to directly address this issue with spatiotemporal precision. When cRO was decaged on only the left side of the prospective gut tube just prior to looping, all embryos (n=20) retained the normal direction of midgut curvature. Compared with non-irradiated controls (Fig. 4A), however, the average degree of curvature was slightly exaggerated (Fig. 4B,D; $P<0.05$), a result consistent with a reduced ratio of left to right side elongation. By contrast, 52% (n=25) of embryos with cRO decaged on the right side exhibited a significantly less curved midgut compared with non-irradiated controls (Fig. 4C,D; $P<0.01$), a phenotype consistent with more equal tissue elongation on the two sides. Strikingly, in 40% of cases (n=25), right side Rho kinase inhibition even reversed the direction of the midgut curvature (Fig. 4C, inset). These data raise the intriguing possibility that late-stage left-right differences in Rho-mediated tissue elongation shape the curvature of the looping gut tube.

Our results demonstrate the power of light-controlled small-molecule inhibitors to provide novel insight into development without laborious injections or transgenesis. The use of cRO might facilitate investigations in regenerating neurons, stem cell environments, engineered tissues, organ culture or other contexts in which localized Rho signaling is relevant. Moreover, because most type I kinase inhibitors (Zhang et al., 2009) have a core heterocyclic scaffold that is amenable to installation of NPOM, photocaging might be a generalizable strategy for creating loss-of-function reagents for numerous signaling pathways. The elegant combination of light control with the tuneability and cross-species efficacy of pharmacology will make caged inhibitors widely applicable in multiple developmental contexts.

Competing interests statement
The authors declare no competing financial interests.

Supplementary material
Supplementary material available online at
http://dev.biologists.org/lookup/suppl/doi:10.1242/dev.072165/-/DC1

References
Aznar, S., Fernandez-Valeron, P., Espina, C. and Lacal, J. C. (2004). Rho GTPases: potential candidates for anticancer therapy. *Cancer Lett.* **206**, 181-191.
Cadotte, D. W. and Fehlings, M. G. (2011). Spinal cord injury: a systematic review of current treatment options. *Clin. Orthop. Relat. Res.* **469**, 732-741.
Cambridge, S. B., Geissler, D., Calegari, F., Anastassiadis, K., Hasan, M. T., Stewart, A. F., Huttner, W. B., Hagen, V. and Bonhoeffer, T. (2009). Doxycycline-dependent photoactivated gene expression in eukaryotic systems. *Nat. Methods* **6**, 527-531.
Deiters, A. (2010). Principles and applications of the photochemical control of cellular processes. *Chembiochem.* **11**, 47-53.
Deiters, A., Garner, R. A., Lusic, H., Govan, J. M., Dush, M., Nascone-Yoder, N. M. and Yoder, J. A. (2010). Photocaged morpholino oligomers for the light-

regulation of gene function in zebrafish and *Xenopus* embryos. *J. Am. Chem. Soc.* **132**, 15644-15650.

Ellis-Davies, G. C. (2007). Caged compounds: photorelease technology for control of cellular chemistry and physiology. *Nat. Methods* **4**, 619-628.

He, L., Wang, X., Tang, H. L. and Montell, D. J. (2010). Tissue elongation requires oscillating contractions of a basal actomyosin network. *Nat. Cell Biol.* **12**, 1133-1142.

Ibanes, M. and Izpisua Belmonte, J. C. (2009). Left-right axis determination. *Wiley Interdiscip. Rev. Syst. Biol. Med.* **1**, 210-219.

Kim, G. H. and Han, J. K. (2005). JNK and ROKalpha function in the noncanonical Wnt/RhoA signaling pathway to regulate Xenopus convergent extension movements. *Dev. Dyn.* **232**, 958-968.

Lai, S. L., Chang, C. N., Wang, P. J. and Lee, S. J. (2005). Rho mediates cytokinesis and epiboly via ROCK in zebrafish. *Mol. Reprod. Dev.* **71**, 186-196.

Lusic, H. and Deiters, A. (2006). A new photocaging group for aromatic *N*-heterocycles. *Synthesis* **2006**, 2147-2150.

Lusic, H., Young, D. D., Lively, M. O. and Deiters, A. (2007). Photochemical DNA activation. *Org. Lett.* **9**, 1903-1906.

Mathew, L. K., Sengupta, S., Franzosa, J. A., Perry, J., La Du, J., Andreasen, E. A. and Tanguay, R. L. (2009). Comparative expression profiling reveals an essential role for raldh2 in epimorphic regeneration. *J. Biol. Chem.* **284**, 33642-33653.

Moura, R. S., Coutinho-Borges, J. P., Pacheco, A. P., Damota, P. O. and Correia-Pinto, J. (2011). FGF signaling pathway in the developing chick lung: expression and inhibition studies. *PLoS ONE* **6**, e17660.

Muller, J., Prather, D. and Nascone-Yoder, N. M. (2003). Left-right asymmetric morphogenesis in the *Xenopus* digestive system. *Dev. Dyn.* **228**, 672-682.

Nieuwkoop, P. D. and Faber, J. (1994). *Normal Table of Xenopus laevis (Daudin).* New York: Garland Publishing.

Reed, R., Womble, M. A., Dush, M. K., Tull, R. R., Bloom, S. K., Morckel, A. R., Devlin, E. W. and Nascone-Yoder, N. M. (2009). The morphogenesis of the primitive gut tube is generated by Rho/ROCK/Myosin II-mediated endoderm rearrangements. *Dev. Dyn.* **238**, 3111-3125.

Remond, M. C., Fee, J. A., Elson, E. L. and Taber, L. A. (2006). Myosin-based contraction is not necessary for cardiac c-looping in the chick embryo. *Anat. Embryol. (Berl.)* **211**, 443-454.

Riento, K. and Ridley, A. J. (2003). Rocks: multifunctional kinases in cell behaviour. *Nat. Rev. Mol. Cell Biol.* **4**, 446-456.

Rizzino, A. (2010). Stimulating progress in regenerative medicine: improving the cloning and recovery of cryopreserved human pluripotent stem cells with ROCK inhibitors. *Regen. Med.* **5**, 799-807.

Sherrard, K., Robin, F., Lemaire, P. and Munro, E. (2010). Sequential activation of apical and basolateral contractility drives ascidian endoderm invagination. *Curr. Biol.* **20**, 1499-1510.

Shestopalov, I. A., Sinha, S. and Chen, J. K. (2007). Light-controlled gene silencing in zebrafish embryos. *Nat. Chem. Biol.* **3**, 650-651.

Simoes, S. M., Blankenship, J. T., Weitz, O., Farrell, D. L., Tamada, M., Fernandez-Gonzalez, R. and Zallen, J. A. (2010). Rho-kinase directs Bazooka/Par-3 planar polarity during Drosophila axis elongation. *Dev. Cell* **19**, 377-388.

Sinha, D. K., Neveu, P., Gagey, N., Aujard, I., Benbrahim-Bouzidi, C., Le Saux, T., Rampon, C., Gauron, C., Goetz, B., Dubruille, S. et al. (2010). Photocontrol of protein activity in cultured cells and zebrafish with one- and two-photon illumination. *Chembiochem.* **11**, 653-663.

Sive, H. L., Grainger, R. M. and Harland, R. M. (1998). *Early Development of Xenopus laevis.* Cold Spring Harbor, New York: Cold Spring Harbor Laboratory Press.

Tamura, M., Nakao, H., Yoshizaki, H., Shiratsuchi, M., Shigyo, H., Yamada, H., Ozawa, T., Totsuka, J. and Hidaka, H. (2005). Development of specific Rho-kinase inhibitors and their clinical application. *Biochim. Biophys. Acta* **1754**, 245-252.

Thumkeo, D., Shimizu, Y., Sakamoto, S., Yamada, S. and Narumiya, S. (2005). ROCK-I and ROCK-II cooperatively regulate closure of eyelid and ventral body wall in mouse embryo. *Genes Cells* **10**, 825-834.

Wacker, S. A., Oswald, F., Wiedenmann, J. and Knochel, W. (2007). A green to red photoconvertible protein as an analyzing tool for early vertebrate development. *Dev. Dyn.* **236**, 473-480.

Wang, X., He, L., Wu, Y. I., Hahn, K. M. and Montell, D. J. (2010). Light-mediated activation reveals a key role for Rac in collective guidance of cell movement in vivo. *Nat. Cell Biol.* **12**, 591-597.

Watanabe, M. (2010). Regeneration of optic nerve fibers of adult mammals. *Dev. Growth Differ.* **52**, 567-576.

Wei, L., Roberts, W., Wang, L., Yamada, M., Zhang, S., Zhao, Z., Rivkees, S. A., Schwartz, R. J. and Imanaka-Yoshida, K. (2001). Rho kinases play an obligatory role in vertebrate embryonic organogenesis. *Development* **128**, 2953-2962.

Yarrow, J. C., Totsukawa, G., Charras, G. T. and Mitchison, T. J. (2005). Screening for cell migration inhibitors via automated microscopy reveals a Rho-kinase inhibitor. *Chem. Biol.* **12**, 385-395.

Zhang, J., Yang, P. L. and Gray, N. S. (2009). Targeting cancer with small molecule kinase inhibitors. *Nat. Rev. Cancer* **9**, 28-39.
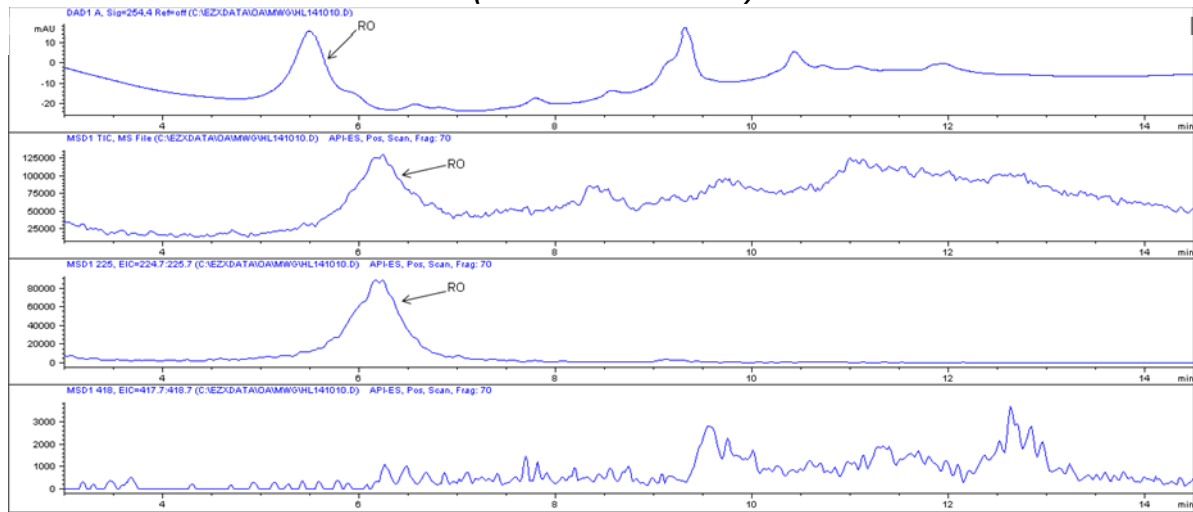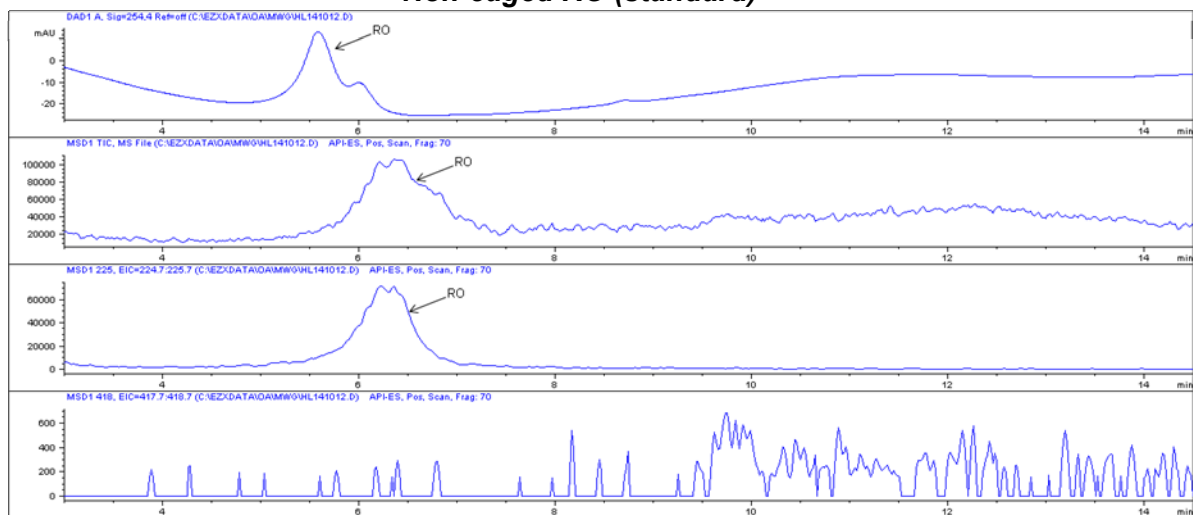
H₂O

DMSO

TMS

ppm (f1)   10.0   5.0   0.0

H₂O

DMSO

TMS

ppm (f1)   10.0   5.0   0.0
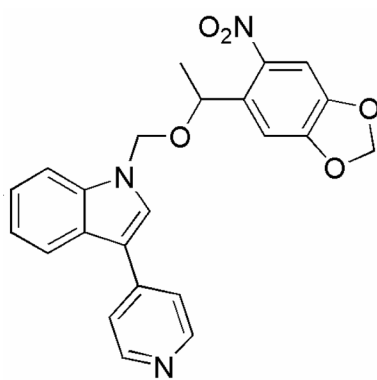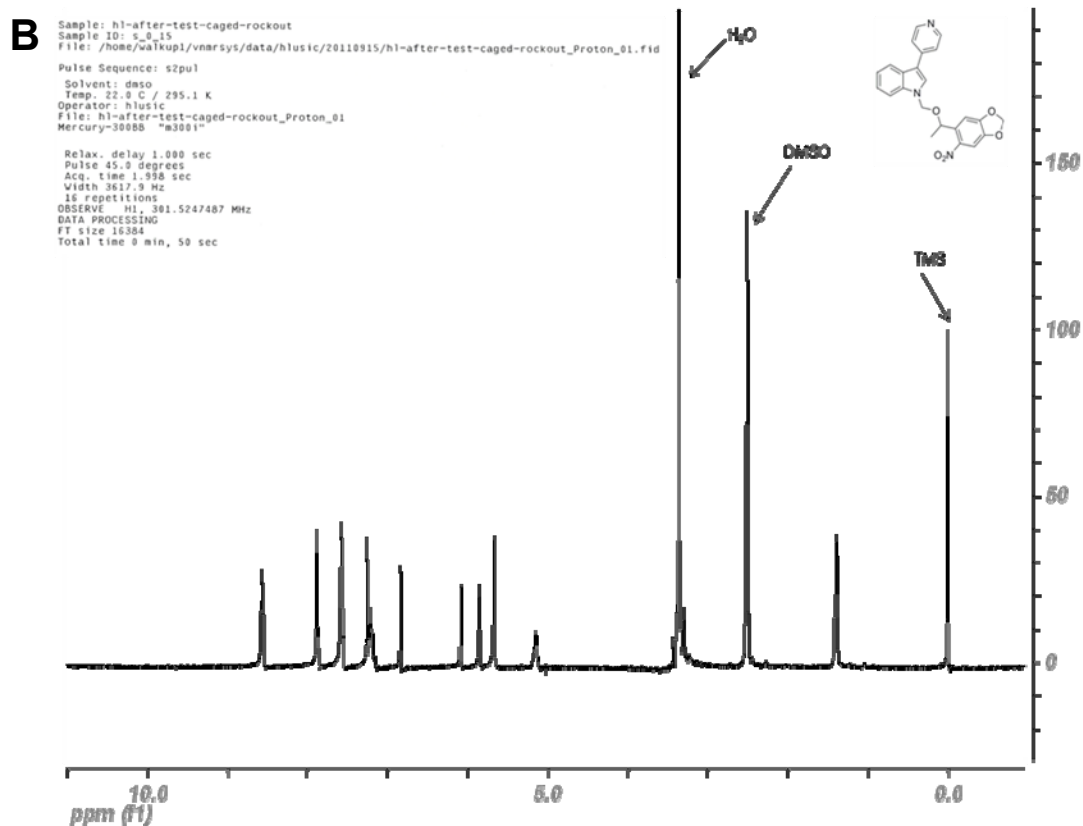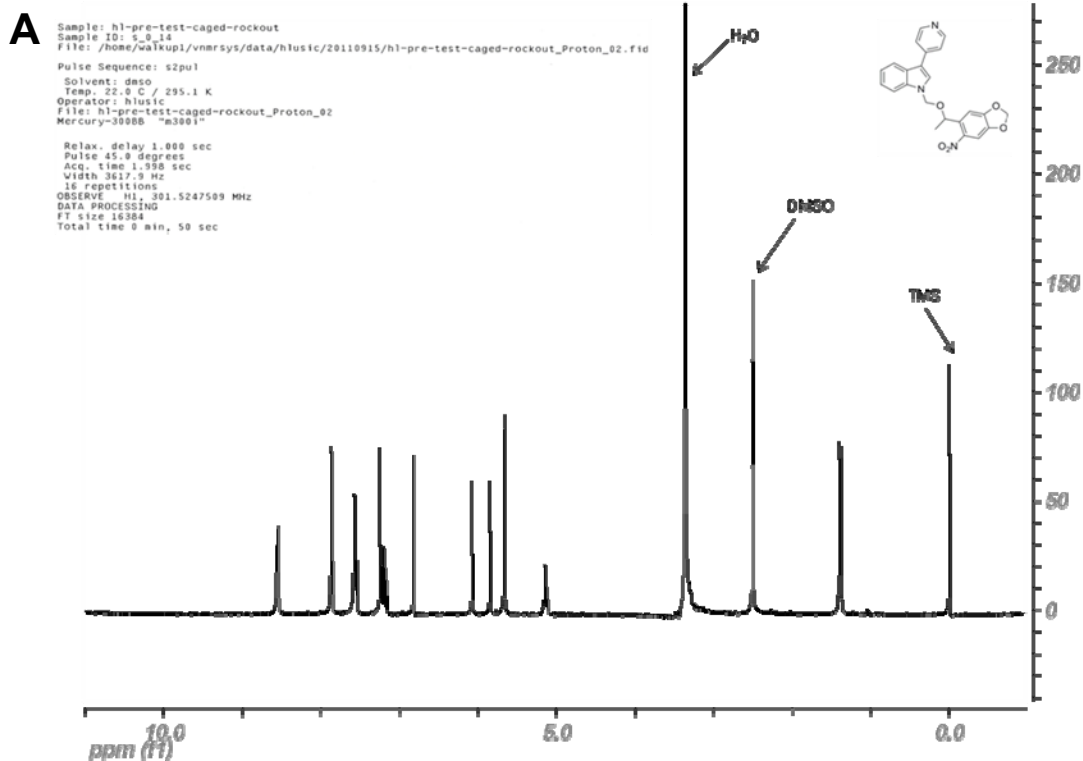
cRO (before UV irradiation)

A
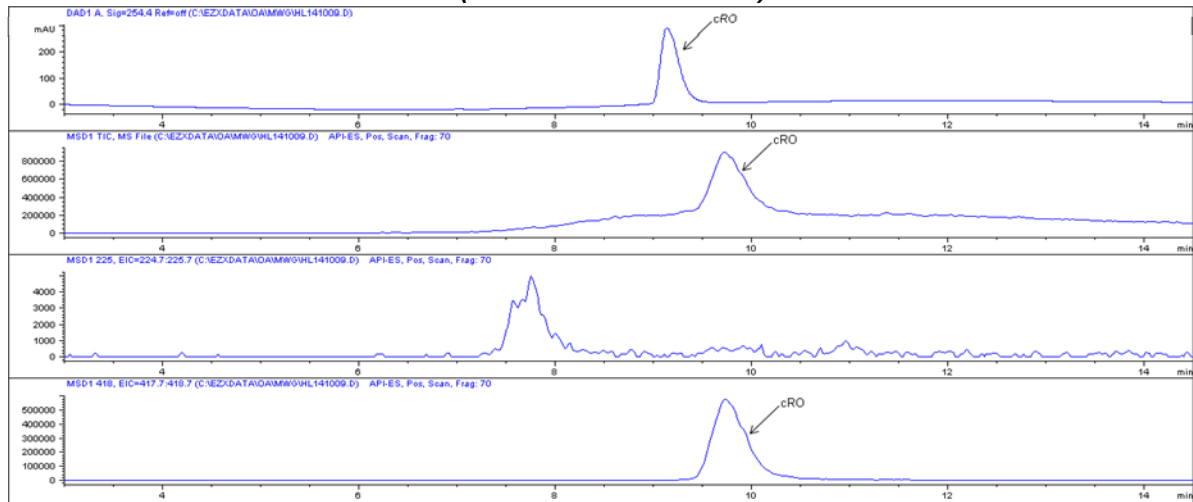
cRO (after UV irradiation)

B

Non-caged RO (standard)

C

untxt (no UV)

DMSO (no UV)

DMSO (+ UV)

cRO (no UV)

cRO (+ UV)
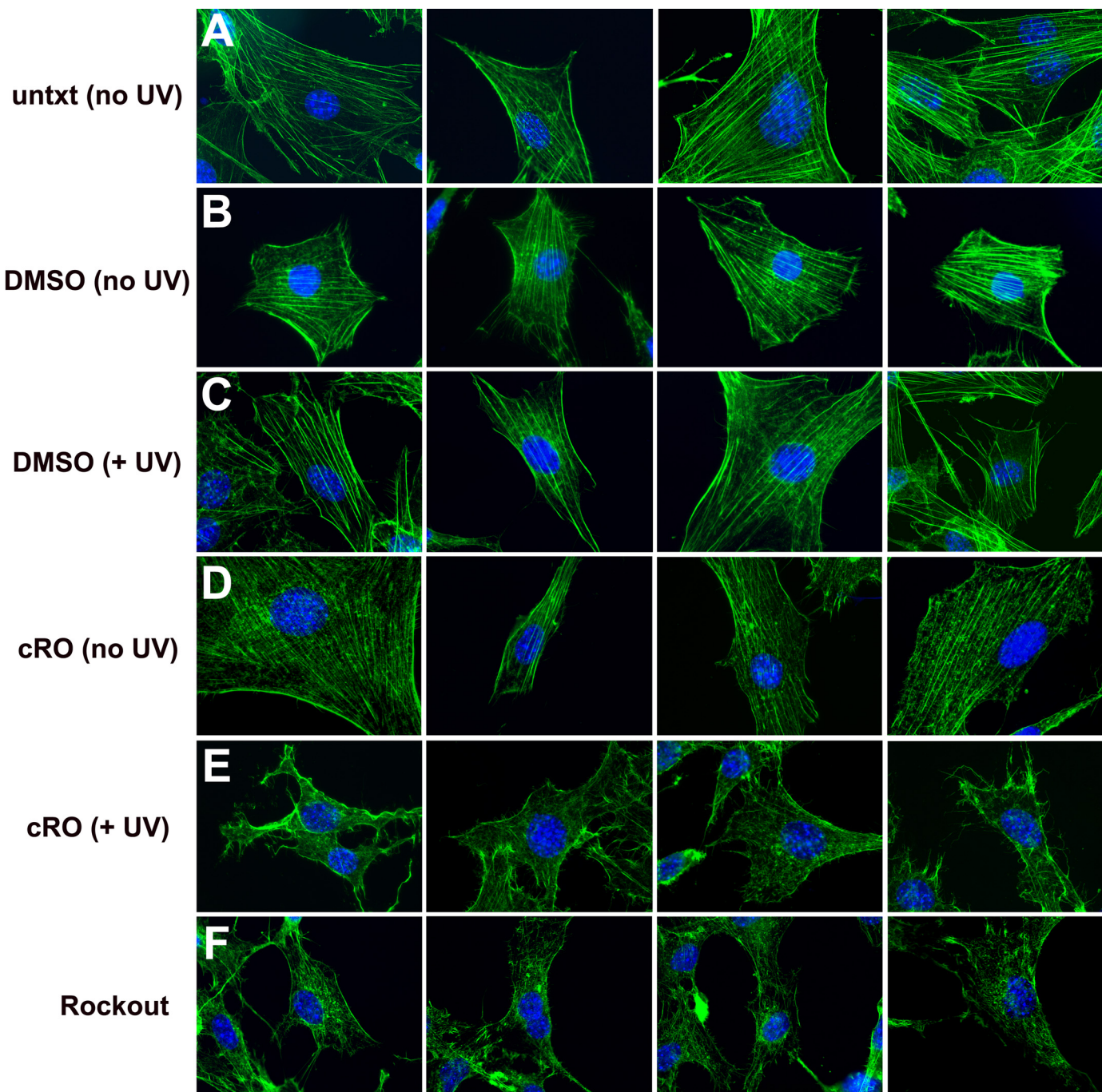
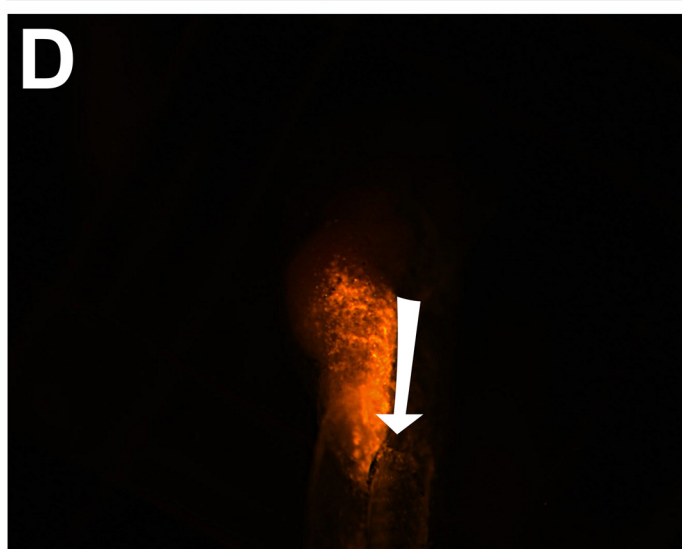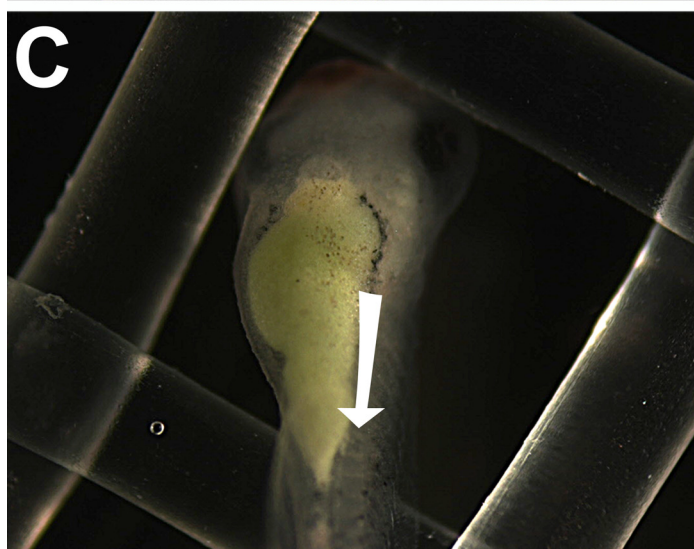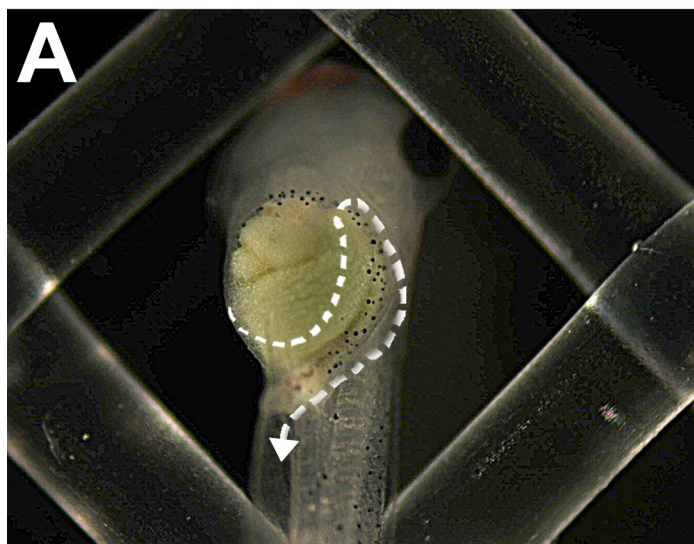Rockout

Table S1. The relative intra-embryonic concentrations of caged Rockout (cRO) and decaged Rockout (RO) as determined by liquid chromatography/mass spectrometry (LC/MS)

Exposure	Stage	RO (nM)	cRO (nM)
Media alone	38	NF	<100
Solvent (–UV)	38	<10	<120
Solvent (+UV)	38	<10	<100
15 μM cRO (–UV)	38	16[¶]	45173[*,#]
15 μM cRO (+UV)[§]	38	275[‡,¶]	5357[#]
Media alone	45	NF	<100
Solvent (–UV)	45	<10	<100
Solvent (+UV)	45	<10	<250
15 μM cRO (–UV)	45	94**	11965[*,‡‡]
15 μM cRO (+UV)[§]	45	1321[‡,**]	1068[‡‡]

Tailbud stage embryos (stage 37) were cultured in medium plus the indicated compounds for 2 hours, rinsed and then kept in the dark or subjected to 1 minute 365 nm decaging (+UV). For each condition, whole embryos were harvested immediately after uptake and decaging (stage 38) or were cultured in media alone and guts were dissected at the completion of gut morphogenesis (stage 45). For LC/MS, excess medium was removed and the tissues from ten embryos were pooled and dissolved in acetonitrile with three cycles of freeze-thaw plus vortex agitation. The acetonitrile extracts were then spun at full speed in a microcentrifuge at 4°C for 5 minutes. The clear supernatant was analyzed by LC/MS at the NCSU Genomic Sciences Laboratory.

*The lower concentration of cRO at stage 45 versus stage 38 reflects its gradual diffusion out of the embryo during culture in media alone.

‡The higher concentration of RO observed at stage 45 versus stage 38 reflects its enrichment in the dissected gut tissues.

§+UV samples were irradiated on only the right-hand side of the prospective gut tube; thus, cRO is expected to be only partially decaged.

¶Concentration of RO in +UV sample is 17-fold higher than in –UV.

#Concentration of cRO in +UV sample is decreased by 88% compared with –UV.

**Concentration of RO in +UV sample is 14-fold higher than in –UV.

‡‡Concentration of cRO in +UV sample is decreased by 91% compared with –UV.

NF, not found.